Design, Simulation and Modeling of LTCC based Micro Hotplate for Gas Sensor Applications

Dheeraj Kharbanda, P.K. Khanna, Chandra Shekhar
CSIR-Central Electronics Engineering Research Institute,
Pilani, India
E-mail:dheeraj.kharbanda@gmail.com

Anand Mohan
National Institute of Technology,
Kurukshetra, India

Abstract— **Low temperature co-fired ceramics (LTCC)-technology, which is widely used for packaging and manufacturing high frequency RF components, is used for fabrication of micro-hotplates (MHP). Gas sensors produced using this technology leads to low power consumption (500 mW for 226 °C) due to low thermal conductivity (3-4 W/(m-K)). For small series, this technology is remarkably inexpensive compared to the expensive silicon technology. Thermal properties such as temperature distribution and power consumption have been investigated using FEM (Finite Element Method) simulations. Mathematical modeling of these hotplates is also done in accordance with the simulated results.**

Keywords- Low temperature co-fired ceramics (LTCC); micro hot-plate (MHP); Finite Element Method (FEM); ANSYS; Gas sensor

I. INTRODUCTION

Gas sensors based on metal-oxide films are mainly manufactured by two different technologies. One is the Thick film technology known from a long time in which the heater and conductor tracks are screen printed on the front and the back side of the ceramic substrate. The gas sensing layer is deposited over the electrodes. These sensors are stable at high range of temperatures [1-4]. The technology is inexpensive and batch fabrication can be done in a cost effective manner. The large size of the device leads to high power consumption [5,6].

The other one is silicon gas sensors which were introduced using micro-machining technology. Selecting an appropriate geometry and suspending the hot-plate by thin beams on a frame leads to low power consumption. Due to the cavity formation, large conductive losses were avoided [7, 8]. But the technology is quite expensive for manufacturing of small series and also the silicon gas sensors shows poor high temperature stability.

LTCC technology allows us to combine the advantages of both technologies to fabricate a low power, high temperature stable, and inexpensive gas sensor [9, 10]. This advantage lies with the low thermal conductivity of LTCC materials (3-4 W/m-K) [11]. The possibility to structure unfired tapes offers fabrication of any desired shape of heater. The parallel processing of LTCC technology results in decreasing the overall fabrication time.

.

II. DESIGNING AND SIMULATIONS

Closed membrane and suspended membrane structures shown in Fig. 1 were compared and suspended membrane was opted for further designing due to its advantages listed in Table 1. The cavities present in the suspended membrane type structure reduce its thermal mass which further reduces the losses. These cavities also help in circulation of air to maintain low temperature of the outer frame.
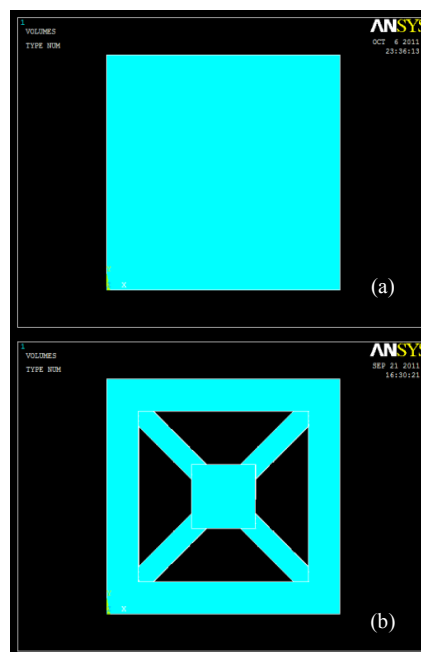

Figure 1. Types of structures (a) Closed Membrane (b) Suspended Membrane

TABLE I.   Closed Membrane vs. Suspended Membrane type structures

Closed Membrane	Suspended Membrane
More thermal mass	Less thermal mass
More losses	Less losses
High temperature around the boundaries	Low frame temperature

FEM simulations using ANSYS were done to decide the geometry of the heater. The thickness of the MHP was kept 305 μm. Line width of the heater was kept 200 μm due to the constraints in the printing technology. Keeping the membrane area and the resistance to be constant, simulations were done at 2.5 V for both the heater geometries viz. meander and double spiral as shown in Fig.2. The membrane area was kept 14.44 mm^2 and the initial resistance was 12.5 Ω. The outer frame size was fixed at 15 mm x 15 mm. The sheet resistivity for the platinum was taken as 100 mΩ. The double spiral heater printed at 14.44 mm^2 area can be accommodated in 11.56 mm^2 of membrane area which further increases the temperature for same power. The membrane size of the MHP was fixed to 3.4 mm x 3.4 mm and the dimensions of outer frame were also varied as 11 mm x 11 mm, 15 mm x 15 mm and 25 mm x 25 mm respectively. The beam width was kept 1mm. Simulations were done using parameters listed in Table 2 and the results are shown in Fig.3

TABLE 2.   Parameters used during simulation and modeling

Material Properties	LTCC	Platinum	Gold
Thermal Conductivity (W/(m-K))	3	72	310
Resistivity (ohm-m)	>10^{10}	1.05x10^{-5}	2.2x10^{-8}
Specific Heat (J/kg/K)	729	133	129
Density (kg/m^3)	3100	21450	19300
Young's Modulus (Gpa)	152	168	79
Poisson's Ratio	0.24	0.38	0.44
Thermal expansion (1/K)	5.8x10^{-6}	8.9x10^{-6}	14.2x10^{-6}
Convection coefficient (h)	25	23	-

III.   RESULTS AND DISCUSSIONS

Double Spiral heater showed 1.38°C of extra temperature over meander shape at the same voltage i.e. 2.5 V. The output is shown in Fig.2. For the structures with frame sizes shown in Fig. 3, the number of hotplates that could be fabricated in a 3" x 3" LTCC substrate is 16, 9 and 4 respectively. But for 11 mm x 11 mm frame size the temperature achieved is lower at same power consumption (184 $^{\circ}$C at 0.5 W) than that of 15 mm x 15 mm frame (226 $^{\circ}$C at 0.5 W). The power consumption is least for 25 mm x 25 mm frame size (261 $^{\circ}$C at 0.5 W) but we can have only 4 hot-plates in the given size. So, the outer frame size was set to 15 mm x 15 mm.
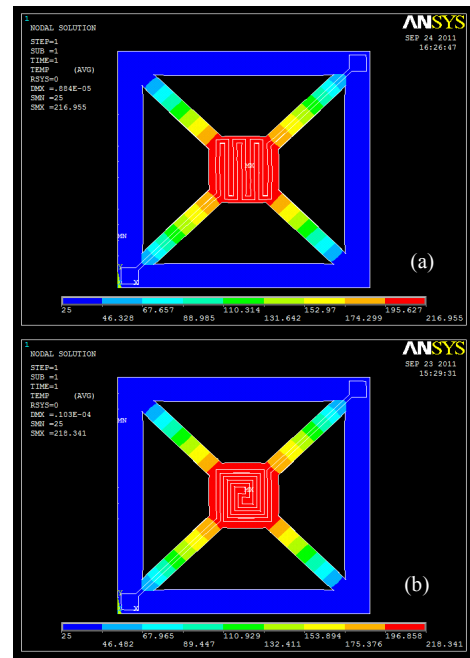

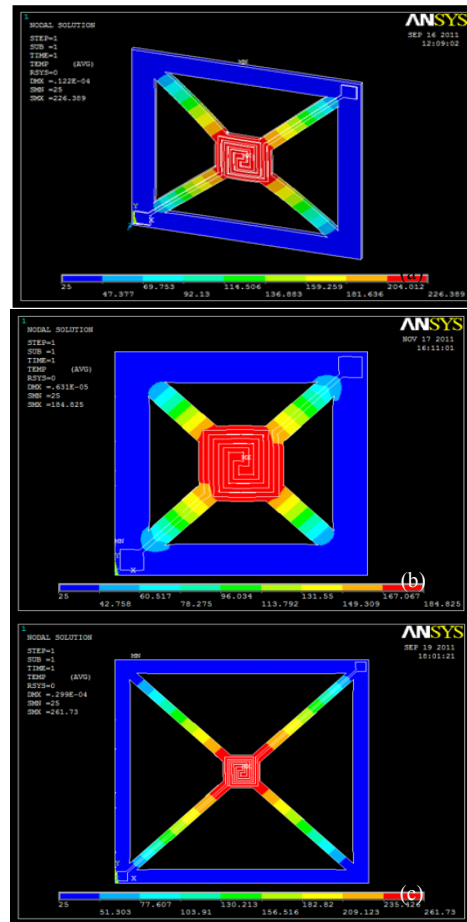Figure 2. Heater Geometries (a) Meander (b) Double Spiral

Figure 3. Simulated results of Micro-hotplate structure with outer frame sizes (a) 11mm x 11 mm, (b) 15 mm x 15 mm and (c) 25 mm x25 mm

IV. MATHEMATICAL MODELING OF MICRO HOT-PLATE

The modeling presented here gives an idea about the temperature which could be achieved using a particular membrane size of given MHP. But this model could not distinguish the change done in the outer frame size of the MHP. Changes made in outer frame size can be analyzed by FEM simulations as discussed above.

The input power supplied to the heater is P_{in}:

$$P_{in} = V_{in}^2/R = V_{in}^2.A/\rho L \qquad (1)$$

Where V_{in} is the applied voltage, R is the resistance of the heater, ρ is the resistivity, L is the length and A is the cross sectional area of the heater element. Also for Platinum the resistivity varies with temperature and hence the resistance changes. Therefore the P_{in} can be written as

$$P_{in} = V_{in}^2/R_0 (1+\alpha \Delta T) \qquad (2)$$

Where α is TCR (temperature coefficient of resistivity) of platinum. Its value is 0.0037 per $^\circ$C. The heat dissipated on the MHP is due to the heat conduction from the membrane towards the outer frame, and convection losses to the surroundings and heat losses due to radiation.

A. Conduction losses: These losses can be represented as

$$P_{cond} = 4KA (\Delta T/\Delta x) \qquad (3)$$

Where K is the thermal conductivity in W/m-K, A is the cross sectional area of the membrane and Δx is the length of the beams over which there is a loss.

B. Convection losses: They are given by

$$P_{conv} = h.A.\Delta T \qquad (4)$$

Where h is the convection coefficient, A is the cross sectional area and ΔT is the change in temperature.

C. Radiation losses: These losses are given as

$$P_{rad} = \sigma\varepsilon A (T^4-T_s^4) = \sigma\varepsilon A\Delta T^4 \qquad (5)$$

Where σ (= 5.67 x 10^{-8} Wm^{-2}K^{-4}) is Stefan-Boltzmann constant and ε is emissivity whose value lies between 0 and 1, depending upon the surface composition. From (3), (4) and (5) the total power dissipated (P_{disp}) is

$$P_{disp} = P_{cond} + P_{conv} + P_{rad} \qquad (6)$$

Hence the total effective power available for heating the resistance is

$$P_{eff} = P_{in} - (P_{cond} + P_{conv} + P_{rad}) \qquad (7)$$

$$P_{eff} \text{ x time} = \Sigma (m.s.\Delta T)$$

$$= m_{LTCC}.s_{LTCC}.\Delta T + m_{Pt}.s_{Pt}.\Delta T + m_{Au}.s_{Au}.\Delta T \qquad (8)$$
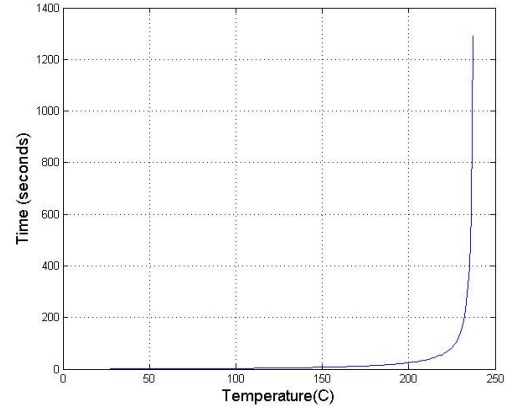

Figure 4. Temperature vs. Time Plot

Where m_{LTCC}, m_{Pt}, m_{Au} are the mass of LTCC, Platinum and Gold and s_{LTCC}, s_{Pt}, s_{Au} are the specific heat of the materials respectively. Mass of the material can be calculated by knowing its density and volume. Using this model we can calculate the temperature at a particular voltage. For 2.5 V and 3.4 mm x 3.4 mm of the membrane size we will get 237 $^\circ$C irrespective of the outer frame size of the hot-plate. The result is depicted in Fig. 4.

V. CONCLUSIONS

Double spiral heater geometry is preferred over meander shaped geometry because of extra temperature observed. Optimum result in terms of power and also the number of hotplates that can be produced using 3"x 3" LTCC substrate were obtained with outer frame size 15mm and membrane size as 3.4 mm x 3.4 mm. The mathematical modeling gives an idea about the temperature that could be achieved using a particular membrane size of given MHP.

REFERENCES

[1] R. Moos, R. Müller, C. Plog, A. Knezevic, H. Leye, E. Irion, T.Braun, K.-J. Marquardt, K. Binder, "Selective ammonia exhaust gassensor for automotive applications", Sens. Actuators B 83 181–189, 2002.

[2] A. Takami, "Development of titania heated exhaust-gas oxygen sensor", Ceram. Bull. 67, 1956–1960, 1988.

[3] R. Moos, F. Rettig, A. Hürland, C. Plog, Temperature-independent resistive oxygen exhaust gas sensor for lean-burn engines in thick-film technology, Sens. Actuators B 93 , 42–49, 2003.

[4] I. Denk, K. Ingrisch, T. Weigold, H. Baumann, K. Weiblen, B. Zeppenfeld, B. Schumann, "New CO/NOx-sensorsystem for automotive climate control in a small-size housing with high mounting flexibility", SENSOR 99 Proceedings, Nürnberg, pp 339–344, 1999.

[5] H. Zheng, O.T. Sørensen, "Integrated oxygen sensors based on Mg doped SrTiO3 fabricated by screen-printing", Sens. Actuators B 65, 299–301, 2000.

[6] I. Simon, N. Barsan, M. Bauer, U. Weimar, "Micromachined metaloxide gas sensors: opportunities to improve sensor performance", Sens. Actuators B 73 1–26, 2001.

[7] S.K. Fung, Z. Than, P.C. Chan, J.K. Sin, P.W. Cheung, "Thermalanalysis and design of a micro-hotplate for integrated gas-sensor applications", Sens. Actuators A 54 482–487, 1996.

[8] Y. Mo, Y. Okawa, M. Tajima, N. Takehito, N. Yoshiike, K.Naturkawa, "Micro-machined gas sensor array based on metal filmmicro-heater", Sens. Actuators B 79 175–181, 2001.

[9] S. Astie, A. Gue, E. Scheid, L. Lescouzéres, A. Cassagnes, "Optimization of an integrated SnO2 gas sensor using a FEM simulator", Sens. Actuators A 69 205–211, 1998.

[10] Jaroslaw Kita, Frank Rettig, and Ralf Moos, "Hot Plate Gas Sensor- Are Ceramics Better?", Int. J. Appl. Ceram. Technol., 2 [5] 383–389 , 2005

[11] F. Rettig and R. Moos, ''Ceramic Meso Hot-Plates for Gas Sensors,'' Sensors Actuat. B: Chem., 103, 91–97, 2004.